Inhibition of ACSS2-mediated H3K9 crotonylation alleviates kidney fibrosis via IL-1β-dependent macrophage activation and tubular cell senescence

Lingzhi Li
West China Hospital of Sichuan University

Ting Xiang
West China Hospital of Sichuan University

Yiting Wu
West China Hospital of Sichuan University

Han Feng
Tulane Research and Innovation for Arrhythmia Discoveries- TRIAD Center, Tulane University School of Medicine

Jing Liu
West China Hospital of Sichuan University

Sibei Tao
West China Hospital of Sichuan University

Fan Guo
West China Hospital of Sichuan University

Ping Fu
West China Hospital of Sichuan University

Liang Ma
Liang_m@scu.edu.cn

West China Hospital of Sichuan University   https://orcid.org/0000-0001-8327-7969

Article

Abstract

Histone lysine crotonylation (Kcr), a novel posttranslational modification, is widespread as acetylation (Kac); however, its roles are largely unknown. In this study, we report that histone Kcr of tubular epithelial cells was significantly elevated in fibrotic kidneys. By screening these crotonylated/acetylated factors, a crotonyl-CoA-producing enzyme—ACSS2 (acyl-CoA synthetase short chain family member 2)—was found to remarkably promote histone 3 lysine 9 crotonylation (H3K9cr) without influencing H3K9ac. Combined analysis of ChIP and RNA sequencing revealed that the hub proinflammatory cytokine, IL-1β (which is regulated by H3K9cr), may play a significant role in kidney fibrosis. Genetic and pharmacologic inhibition of ACSS2 both attenuated kidney fibrosis, as well as suppressed H3K9cr-mediated IL-1β expression, which thereby alleviated IL-1β-dependent macrophage activation and tubular cell senescence. Collectively, our findings uncover that H3K9cr plays a critical, previously unrecognized role in kidney fibrosis, where ACSS2 represents an attractive target for strategies that aim to slow fibrotic kidney disease progression.

Introduction

Chronic kidney disease (CKD) is a condition characterized by functional deterioration with sustained inflammation, and progressive fibrosis of the kidneys, affecting over 800 million people worldwide [1,2]. As known, macrophage activation is a common feature of inflammation in active fibrotic kidney lesions. And accelerated tubular cell senescence via the release of components of senescence-associated secretory phenotypes (SASPs) also promote the pathogenesis of kidney fibrosis. Since current treatments to slow CKD progression are limited and nonspecific, it eventually progress to end-stage kidney disease, which requires dialysis or kidney transplantation [3]. Therefore, exploring the precise mechanisms of CKD to find potential drug targets is of great importance to ultimately arrest and prevent its progression.

Protein posttranslational modifications (PTMs) play essential roles in modifying protein function and thus influence numerous biological processes, including organismal development, cell differentiation, cell death, and inflammation [4]. The aberrant PTMs in fibrosis and inflammation are becoming more important in the progression of CKD [5]. Histone lysine acetylation (Kac) is one of the most well-studied histone PTMs. With the development of mass spectrometry (MS) techniques [6,7], lysine crotonylation (Kcr) was found to be a novel evolutionarily conserved PTM principally related to active transcription, where histones are the most abundant crotonylated proteins [8]. Histone Kcr, specifically enriched at promoters and potential enhancers in the mammalian genome, exhibits a stronger effect on transcription than histone Kac; however, Kcr and Kac are catalyzed by several similar enzymes and metabolic states, which makes it difficult to distinguish them and explore the role of crotonylation alone.

In the context of kidney diseases, few studies reported that histone Kcr was observed in both healthy and diseased kidneys—including acute kidney injury (AKI) [8] and IgA nephropathy [9]—suggesting that it may play a role in epigenetic regulation of gene expression in kidney disease. Recently, nuclear condensation of a chromodomain Y-like transcription corepressor (CDYL) has linked histone Kcr to transcriptional

responses and cystogenesis in autosomal dominant polycystic kidney disease (ADPKD). However, there is little knowledge regarding the functional role of histone Kcr relative to Kac during kidney injury and fibrosis.

In this study, we aimed to explore the function of histone crotonylation—especially histone 3 lysine 9 crotonylation (H3K9cr)—in patients and mice with kidney fibrosis and tubular epithelial cells (TECs). Our results revealed that inhibition of H3K9cr alleviated kidney fibrosis by suppressing macrophage activation and senescence of TECs. We propose that the crotonyl-CoA-producing enzyme, acyl-CoA synthetase short chain family member 2 (ACSS2), represents an attractive drug target for strategies to slow fibrotic kidney disease progression.

Results

The expression of histone Kcr positively correlates with the severity of CKD in patients and mice

To explore the roles of protein crotonylation in human kidneys, we first collected kidney biopsy slides and determined the clinical characteristics of patients with CKD, and performed immunohistochemistry (IHC) using antibodies targeting crotonyl lysine (anti-Kcr) (Fig. 1A and Fig. S1A). The results demonstrated that Kcr was mainly present in TECs, and was significantly higher in the kidneys of patients with than without CKD (Fig. 1A). The IHC data showed that the intensity of Kcr staining positively correlated with disease progression, especially samples with nuclear staining (Fig. 1B and Fig. S1B). Kcr participated in CKD as well as contributed to fibrosis in the obstructed kidneys of mice. The immunofluorescence (IF) staining data showed that unilateral ureteric obstructions (UUOs) induced the increasing expression of Kcr, which was mainly colocalized in the nuclei (Fig. 1C).

To confirm the changes in the histone Kcr, we extracted total histones from the fibrotic kidneys of mice and evaluated the histone purification using Coomassie brilliant blue staining and liquid chromatography-mass spectrometry (LC-MS/MS) analysis. The LC-MS/MS analysis confirmed that all the proteins were extracted from the nucleus and functioned with chromatin structure and dynamics (Fig. S2A-C). To compare the levels of histone crotonylation in kidneys, western blotting analysis using anti-Kcr antibodies was performed (Fig. 1D and Fig. S1C), demonstrating that the increase in histone crotonylation was accompanied with kidney fibrosis in both UUO and folic acid nephropathy (FAN) mice (Fig. S2D-G).

As previously reported, different histone lysine modifications might have diverse roles. To identify histone Kcr and Kac at several important histone H3 residues reported (K9, K14, K18, and K27), we used different antibodies to blot the histone extraction. Particularly, H3K9cr increased remarkably in two experimental models of kidney fibrosis, while H3K9ac remained stable (Fig. 1E and Fig. S1D), proposing that H3K9cr may have distinct effects relative to H3K9ac in renal fibrosis. However, H3K18cr and H3K27cr, corresponding with H3K18ac and H3K27ac, both increased in fibrotic kidneys, suggesting that these two markers are coregulated. Most interestingly, H3K14cr increased in kidneys with FAN and UUO; H3K14ac

showed opposite trends, recommending that the roles of histone Kcr and Kac are both complicated and comprehensive (Fig. S2H-K).

Genetic deletion of ACSS2 decreased H3K9 crotonylation and alleviated kidney fibrosis

As histone Kcr and Kac are reversible, dynamic processes mediated by multiple identical enzymes, it has been challenging to distinguish between their individual functions. Based on the abovementioned data, the alterations of H3K9cr appear to be independent of those of H3K9ac in kidney fibrosis. We examined known enzymatic and metabolic regulation variables, including Sirtuin (SirT) 1/2/3/4/5/6 [8,10], histone deacetylase (HDAC) 1/2/3 [11,12], acyl-CoA synthetase short chain family member 2 (ACSS2) [13] and crotonate *in vitro*, to identify critical factors that could regulate H3K9cr more than H3K9ac (Fig. 2A) in both mouse renal tubular epithelial (TCMK-1) cells, and human embryonic kidney (HEK-293T) cells. By screening these factors, ACSS2 overexpression by plasmid transfection (Fig. S3A-B) dramatically increased H3K9cr expression and did not change H3K9ac, indicating that ACSS2 may have a greater impact on H3K9cr than H3K9ac (Fig. S4B).

Crotonate, a recourses of histone Kcr, also increased the expression of H3K9cr and H3K9ac in TECs (Fig. S3C-D, Fig. S4C-D), demonstrating that crotonate has an impact on the histone Kac process via effects on ACSS2. SirT and HDAC were successfully overexpressed in TCMK-1 and HEK-293T cells after transfection with various plasmids (Fig. S3E-P). Overexpression of SirT1/2/3 and HDAC1/2/3 reduced the expression of H3K9cr and H3K9ac in kidney TECs (Fig. S4E-H); however, overexpression of SirT4/5/6 only affected H3K9ac modification without affecting H3K9cr (Fig. S4I-J). Consequently, we purposed that ACSS2, notwithstanding H3K9ac interference, could be the ideal instrument for examining the functions of H3K9cr in TECs.

To understand the role of ACSS2-mediated H3K9cr in renal fibrosis, we generated mice with genetic deletion of ASCC2, taking advantage of the CRISPR/Cas9 knock-out system (Fig. S5A-C). The results of western blotting confirmed ACSS2 reduction in the kidneys of knockout mice (ACSS2$^{-/-}$) compared with littermate controls (Fig. S5D-E). The ACSS2$^{-/-}$ mice were born at the expected Mendelian ratio, with no birth or growth defects and no signs of kidney function defects.

First, two experimental kidney fibrosis mice (with UUOs and FAN) were created using ACSS2$^{-/-}$ mice and littermate controls. After evaluating the expression of H3K9cr by western blotting, we confirmed that genetic knockout of ACSS2 could reduce the expression of H3K9cr in fibrotic kidneys, which was consistent with the results of cell experiments. Similarly, the expression of H3K9ac remained unchanged (Fig. 2B and Fig. S6A-B). Next, we analyzed the phenotype of these animals to explore the function of ACSS2 in kidney fibrosis (Fig. 2A). Histological changes, such as tubule atrophy and interstitial fibrosis, were alleviated in ACSS2$^{-/-}$ compared with wild-type (WT) UUO mice (Fig. 2C). Protein markers of fibrosis, including levels of fibronectin (FN1), collagen type 6 (COL6), and smooth muscle actin (α-SMA),

were higher in fibrotic kidneys, but lower in ACSS2$^{-/-}$ kidneys in UUO mice (Fig. 2D). Transcript levels of fibrotic markers—including Fn1, collagen type 1a1 (Col1a1) and smooth muscle alpha (α)-2 actin (Acta2)—were altered similarly to the levels of fibrotic markers at the protein level (Fig. 2E). Genetic deletion of ACSS2 was confirmed to decrease H3K9cr and alleviate kidney fibrosis in FAN mice (Fig. S6C-F). All these data confirmed that global genetic deletion of ACSS2 would influence H3K9cr expression and thus alleviate kidney fibrosis.

Tubular-specific deletion of ACSS2 decreased H3K9 crotonylation to delay the progression of kidney fibrosis

TECs play a core role in kidney fibrosis [14]. The IHC results confirmed that H3K9cr and ACSS2 was mainly expressed in TECs in fibrotic kidneys (Fig. 3A). To investigate the contribution of ACSS2 in TECs to kidney fibrosis, we crossed ACSS2 flox mice with Ksp-Cre mice to selectively delete ACSS2 in TECs in the kidneys (Fig. S7). The Ksp-Cre ACSS2$^{fl/fl}$ (ACSS2^{tecKO}) mice and Cre-negative littermate controls (ACSS2^{tecWT}) were subjected to UUO or injected with folic acid (FA). The kidneys of ACSS2^{tecKO} and ACSS2^{tecWT} mice exhibited the same extent of H3K9ac when compared with sham-operated kidneys. The H3K9cr expression increased dramatically in ACSS2^{tecWT} UUO kidneys, and was alleviated in ACSS2^{tecKO} UUO kidneys (Fig. 3C). The changes in H3K9cr and H3K9ac were also similar in the kidneys of FAN ACSS2^{tecKO} mice (Fig. S8A).

H&E and Masson staining showed that tubule injury and collagen deposition were alleviated in the kidneys of ACSS2^{tecKO} UUO mice compared with ACSS2^{tecWT} UUO mice (Fig. 3D). The western blot and qPCR results also confirmed that kidney fibrosis in UUO and FAN mice were ameliorated in ACSS2^{tecKO} mice compared with ACSS2^{tecWT} mice, demonstrated by the decreased expression of fibrotic markers (Fig. 3E-F and Fig. S8B-D). In summary, the data indicated that specific deletion of tubular ACSS2 decreased H3K9 crotonylation to delay the progression of kidney fibrosis.

H3K9cr promoted cytokine production and regulated cytokine-cytokine receptor interaction in fibrotic kidneys

Since the genomic locations of H3K9cr have not been previously mapped in kidneys, it is difficult to explore the possible regulatory genes of H3K9cr through the public database. Therefore, we sought to determine the effects of H3K9cr ourselves using chromatin immunoprecipitation sequencing (ChIP-seq). For comparison and as a control, we also performed H3K9ac ChIP-seq using the same samples (Fig. 4A). We found that both H3K9ac and H3K9cr are enriched at transcriptional start sites (Fig. S9). The location of H3K9cr at transcriptional start sites is consistent with previous findings [15,16]. Remarkably, the ChIP signal did not differ between H3K9cr and H3K9ac for control mice, while the ChIP signal of H3K9cr was obviously stronger than that of H3K9ac in the kidneys of UUO mice (Fig. 4C).

We also performed RNA-seq on these samples, as the combination of ChIP-seq and RNA-seq data can be used to decipher the transcriptional regulation network (Fig. 4A). Whether in control mice or mice with kidney fibrosis, the results of individual analyses revealed a strong correlation between H3K9cr and H3K9ac regarding gene expression during the process of kidney fibrosis. The highest quartiles of gene expression displayed the highest occupancy of histone Kac and Kcr, suggesting that both H3K9cr and H3K9ac can activate gene transcription (Fig. 4B).

To further examine the relationship between H3K9cr and H3K9ac, we examined the relative ratio of H3K9cr to H3K9ac when both acylations can be detected (Fig. 4D). This analysis demonstrated that gene expression in UUO kidneys were among those with the highest H3K9 crotonylation/ acetylation ratios. When deleting ACSS2 in UUO kidneys, the decrease in H3K9cr leads to lower H3K9cr/ ac ratios. Nevertheless, deletion of ACSS2 had an insignificant effect on genes in control kidneys, as the H3K9cr levels remained unchanged (Fig. S10A). According to these findings, H3K9cr may activate gene expression similarly to H3K9ac, while having a greater impact on renal fibrosis-related genes.

To understand the specific regulatory genes of H3K9cr in kidney fibrosis, we investigated the RNA-seq data between control and UUO kidneys. Gene Ontology (GO) and Kyoto Encyclopedia of Genes and Genomes (KEGG) pathway studies revealed considerably enriched pathways of cytokine-cytokine receptor interaction, and a cytokine-mediated signaling pathway in fibrotic kidneys (Fig. S10B-C). After ACSS2 deletion in mice, these two pathways decreased (Fig. S10D-E). Furthermore, to determine whether the reduction of the two signaling pathways produced by ACSS2 deletion is regulated by H3K9cr or H3K9ac, we investigated the results of GO pathway analysis from ChIP-seq data. It is noteworthy that the deletion of ACSS2 had a greater impact on the genes controlling cytokine production by H3K9cr than H3K9ac in UUO kidneys (Fig. 4E), which raises the possibility that the renoprotection offered by the deletion of ACSS2 mainly depends on H3K9cr-mediated cytokine production.

Within these pathways, interleukin-1 (IL-1β) was found to be a core and altered proinflammatory cytokine, as mentioned in a previous study [17]. Excitingly, Il1b and Il1r1 displayed increased H3K9cr levels at their proximal promoter regions, and downregulated expression with ACSS2 deletion in UUO kidneys. However, these two genes displayed lower H3K9ac levels and fewer alterations after ACSS2 deletion (Fig. 4F and Fig. S10G). The increase in Il1b and Il1r1 enrichment of H3K9cr following transfection of the ACSS2 plasmid in HEK-293T cells was further confirmed by ChIP-qPCR (Fig. S10H). Overall, our findings indicate that H3K9cr—not H3K9ac—controlled the interaction between cytokines and cytokine receptors (particularly Il1b, which was crucial for fibrotic kidneys).

H3K9 crotonylation promoted IL-1β production in both kidney cells and fibrotic kidneys

As abovementioned, ChIP investigations indicated that IL-1β could be directly regulated by H3K9 crotonylation. We independently evaluated H3K9cr-mediated changes in IL-1β production in animals and cells (Fig. 5A). First, the increase in IL-1β was accompanied by an increase H3K9cr in the fibrotic kidneys

of UUO and FAN mice (Fig. 5B and Fig. S11A-B). When global or tubular specific knockout of ACSS2 were applied to decrease H3K9cr modification in mice with kidney fibrosis, both the protein levels and transcription of IL-1β were suppressed (Fig. 5D-E and Fig. S11C-D). Remarkably, it was clear that the deletion of ACSS2 reduced the amount of IL-1β produced in UUO kidneys, without influencing serum concentration (Fig. 5C).

After demonstrating the alterations of H3K9cr-mediated IL-1β *in vivo*, we used two different kidney cell lines to confirm the link between H3K9cr and IL-1β *in vitro*. Both the protein and mRNA levels of IL-1β noticeably increased following crotonate stimulation (Fig. S12A-D). The expression of IL-1β was further boosted by transfecting TCMK-1 cells with the ACSS2 plasmid, which raises H3K9cr. In addition to intracellular IL-1β, ELISA kit analysis revealed that the concentration of IL-1β in the supernatant of ACSS2-overexpressed TCMK-1 cells was also elevated (Fig. S12E-G); HEK-293T cells showed similar effects (Fig. S12H-J). When SirT1/2/3 and HDAC1/2/3 were overexpressed in TCMK-1 and HEK-293T cells to block H3K9cr modification, the levels of IL-1β decreased (Fig. S13). Surprisingly, IL-1β expression was unaffected by SirT4/5/6 plasmids, which had no impact on H3K9cr alteration (Fig. S14). Collectively, our findings show that whether *in vivo* or *in vitro*, H3K9cr expression is significantly associated with IL-1β production; additionally, ACSS2 may be a key factor to regulate H3K9cr-mediated IL-1β production.

H3K9cr-derived IL-1β promoted macrophage activation in cells and fibrotic kidneys

As known, macrophages (particularly M1 macrophages) are considered deleterious in kidneys, as they sustain the proinflammatory environment, leading to the progression of renal injury and development of fibrosis [18]. IL-1β is an important cytokine that can induce proinflammatory or activated M1 macrophages; thus, it is possible that H3K9cr-mediated IL-1β triggers macrophage activation to promote kidney fibrosis progression.

To test whether IL-1β could promote macrophage polarization, we first stimulated RAW264.7 with different doses of IL-1β; according to the Cell Counting Kit-8 assay, low doses of IL-1β can promote macrophage proliferation (Fig. S15A). As expected, microscopic images depicted changes in cell morphology from a rounded M0 to flat M1 phenotype after IL-1β simulation (Fig. S15B). Additionally, there were significantly higher levels of M1 macrophage markers (Tnf-α, iNOS, and Il1b), and lower levels of M2 markers (CD206) in IL-1β-simulated versus M0 cells; this was consistent with the observed morphological changes (Fig. S15C).

To test whether H3K9cr-derived IL-1β exerted similar effects, we collected the supernatant of HEK-293T cells transfected with ACSS2 plasmids ahead of time to increase H3K9cr, and subsequently stimulated RAW264.7 macrophages (Fig. 6A). After supernatant stimulation, the microscopic images and mRNA levels of M1 macrophage markers—including iNOS, Tnf-α, Mcp1, and Il6—changed, indicating that macrophage polarization occurred (Fig. 6B and Fig. S16A). We repeated the experiments with TCMK-1 cells, and observed similar results (Fig. S16B). In addition to supernatants from ACSS2-overexpressed

cells, we collected supernatants from HEK-293T and TCMK-1 cells transfected with SirT1/2/3 and HDAC1/2/3 plasmids, which inhibited H3K9cr-mediated IL-1β production. Microscopic images revealed that the flat M1 phenotype in the H3K9cr inhibition group was less than in the control group (Fig. S17A). As the previous qPCR tests revealed, H3K9cr inhibition can reduce M1 macrophage markers (Fig. S17B-C).

When observing the M1 macrophage marker *in vivo*, we found that regardless of whether global or tubular epithelial-specific knockout of ACSS2 was performed to decrease H3K9cr modification in mice with kidney fibrosis, Cd68 and Tnf-α were suppressed (Fig. S16C-D). Overall, these data suggest that regulating H3K9cr modification in TECs could influence the secretion of IL-1β, thereby influencing macrophage activation.

H3K9cr-derived IL-1β accelerated tubular cell senescence in cells and fibrotic kidneys

Other than mediating macrophage polarization, recent studies report that IL-1β may be involved in the senescence of several types of cells, including vascular smooth muscle cells [19], astrocytes [20], bovine oviduct epithelial cells [21], mature chondrocytes [22], etc. Recently, several studies have shown positive correlations between senescent cell accumulation and fibrosis in kidneys during ageing [23-25] and disease [26-28]. Based on known results, we suspected that IL-1β—the key mediator identified by H3K9cr—could also regulate TECs senescence in kidney fibrosis.

First, we administered IL-1β directly to TECs at different concentration to determine whether it affected tubular cell senescence. High doses of exogenous IL-1β did not cause any toxicity in TCMK-1 cells, as shown in Fig. S18A; however, even low doses of IL-1β triggered senescence-associated β-galactosidase (SA-β-gal) positive cells (Fig. S18B). IL-1β also increased the cellular senescence marker P53, and several senescence-associated secretory phenotype (SASP) markers (Il6, Mmp9, and Il1b) (Fig. S18C).

To further confirm whether H3K9cr-derived IL-1β has similar effects, we collected supernatants from TCMK-1 cells or HEK-293T cells transfected with ACSS2 plasmids, which are IL-1β enriched. Thereafter, we treated TCMK-1 cells to observe changes in senescence markers. Similarly, the senescence phenotype increased *in vitro*, as evidenced by increased P53, Il6, and Mcp1 levels (Fig. S19A-B). When we evaluated the data *in vivo*, the expression of P53, Il6, and Mcp1 increased in the kidneys of UUO and FAN mice (Fig. S19C-F). Global knockout of ACSS2 in UUO and FAN mice to decrease H3K9cr-mediated IL-1β production resulted in a decrease in P53, Il6, and Mcp1 (Fig. S19G-J). Even when we specifically knocked out ACSS2 in renal TECs, we discovered that the kidney cellular senescence marker decreased significantly (Fig. S19K-L). These data therefore suggest that regulating H3K9cr modification in TECs could influence the secretion of IL-1β and thus influence senescence in TECs.

Anti-IL-1β IgG treatment alleviated macrophage activation and tubular cell senescence in kidney cells and fibrotic kidneys

We attempted to identify approaches to suppress IL-1β after confirming that H3K9cr-generated IL-1β might drive macrophage activation and tubular cell senescence. When anti-IL-1β IgG was added to RAW264.7 cells treated with IL-1β, IL-1β-induced M1 macrophage polarizations and cellular senescence markers P53 and SASP were also diminished (Fig. 6C and E). When treating cells with IL-1β antibodies to neutralize IL-1β-enriched supernatant stimulation, the changes in morphology and mRNA expression of M1 phenotypic markers and cellular senescence could be alleviated (Fig. 6D and F).

To examine the effects of IL-1β *in vivo*, we also administered anti-IL-1β IgG to UUO mice (Fig. 7A). Anti-IL-1β IgG dramatically reduced renal fibrosis in UUO mice, as demonstrated by Masson's trichrome staining and the decreased mRNA and protein expression of kidney fibrosis markers (Fig. 7B-D and Fig. S20A). Anti-IL-1β IgG treatment also suppressed key markers of M1 macrophage and cellular senescence (Fig. 7E-G and Fig. S20B-C). To summarize the data presented above, anti-IL-1β IgG can alleviate M1 macrophage polarization and tubular cellular senescence caused by H3K9cr-mediated IL-1β both *in vivo* and *in vitro*, and thus improve kidney fibrosis.

Pharmacological inhibition of ACSS2 repressed H3K9cr-mediated IL-1β production to protect kidney fibrosis

Although anti-IL-1β IgG can help treat renal fibrosis, monoclonal antibodies are prohibitively expensive for patients with CKD who require long-term treatment. Another option is to use small molecule enzyme inhibitors, which are less expensive and easier to use [29]. Unfortunately, no small molecule inhibitor of IL-1β is available on the market. Importantly, the newly developed ACSS2 inhibitor could serve as an alternative to inhibit IL-1β by reducing H3K9cr modification. In our search to discover a potential therapy, we identified an ACSS2 inhibitor (S8588) [30] that can treat kidney fibrosis mice (Fig. 8A). ACSS2 protein production was inhibited in control mice after seven days of ACSS2 inhibitor administration (Fig. S21A). Inhibiting ACSS2 suppressed H3K9cr, and had no effect on H3K9ac (Fig. 8B and Fig. S21B). Remarkably, the ACSS2 inhibitor (S8588) significantly reduced kidney fibrosis in UUO and FAN mice, as evidenced by improvements in pathological staining, western blot, and qPCR for fibrosis markers (Fig. 8C-D and Fig. S21C-E). As expected, IL-1β decreased after inhibitor treatment, accompanied by a decline in SA-β-gal-positive senescent cells (Fig. 8E-F and Fig. S22A-E). Additionally, the cellular senescence markers P53 and SASP were suppressed (Fig. 8G and Fig. S22G-J). Interestingly, these SASPs could also be identified by M1 macrophages, specifically Il1b, Il6, and Mcp1. The decrease in these inflammatory markers was accompanied by a decrease in the M1 macrophage marker Cd86 (Fig. 8G).

Discussion

Epigenetic regulation—especially histone modification—of gene expression plays a key role in regulating cell fate transitions in the development of various diseases, including kidney fibrosis [31]. However, the newly reported histone Kcr changes and how they affect transcriptional responses in kidney fibrosis remain poorly understood. In this study, the main findings were that overall, increasing H3K9cr was

harmful to kidney fibrosis; the degree of H3K9cr could be modified by ACSS2 to further regulate IL-1β-mediated macrophage activation and tubular cell senescence. This is the first observation demonstrating the potential of the therapeutic manipulation of histone Kcr by ACSS2 inhibition in a kidney fibrosis state.

Despite sharing the same DNA, the kidneys comprise complex tissues of multiple different cell types owing to differential epigenetic modulations that determine the characteristics of each cell type [32]. There is increasing interest in the epigenetic regulation of kidney injury and fibrosis, especially from the viewpoint of chronicity and aging [33]. Constitutive histone Kcr is present in healthy kidneys [7], and increased histone Kcr has been described in ADPKD [34] and AKI induced by FA and cisplatin [8]. As studies of Kcr in the kidneys are rare and immature, the role of Kcr has not been unified. In kidneys with ADPKD, the increased Kcr could be reduced by genetic overexpression of the CDYL and thereby slow cystic growth [34]. However, in FA-induced AKI, crotonate increased histone Kcr and peroxisome proliferator activated receptor coactivator alpha (PGC-1α) expression, thus providing protection against AKI [8]. One of the reasons for the difference in kidney protection or damage effects of histone Kcr may be that researchers use different ways to regulate histone Kcr expression. As we repeatedly emphasized, the same set of enzyme systems are shared by histone Kac and histone Kcr [7,10,11,13]. In our study, we identified and characterized several interventions that regulated H3K9cr in kidneys: genetically changing SirT/ HDAC/ ACSS2 expression and increasing the crotonate substrate availability. We found that several factors, including crotonate but excluding ACSS2, could both influence H3K9cr and regulate H3K9ac expression. Data related to histone Kac has not yet been reported in an AKI study; thus, whether the renoprotective effects of crotonate are based on Kcr or Kac is difficult to differentiate. Moreover, finding a suitable tool to regulate Kcr separately—regardless of whether ACSS2 deletion or CDYL overexpression mice [34] are selected—was challenging. The similar results obtained suggest that histone Kcr-induced kidney injury and inhibited histone Kcr modification may alleviate kidney damage. In another study on the effects of histone Kcr, Kcr regulated gene expression was increased to promote diseases progression [35].

The mechanism by which ACSS2 regulated more H3K9cr than H3K9ac is possibly due to the concentration of crotonyl-CoA and acetyl-CoA [13,36]. Since the intracellular crotonyl-CoA concentration is about 600- to 1,000-fold lower than that of acetyl-CoA, the crotonyl-CoA concentration is likely to be the limiting factor in the crotonyl transfer reaction [13]. Thus, Kcr is more sensitive to any changes that alter cellular crotonyl-CoA levels by the expression/activity/location/interacting partners of crotonyl-CoA-producing enzymes [37]. Identification of signals and transcription factors that induce expression of crotonyl-CoA-producing enzymes, as well as the nuclear interacting partners of these enzymes will be important to further dissect the underlying molecular mechanisms that regulate Kcr during kidney fibrosis.

Given that histone PTMs impact the expression of multiple genes, it remains to be explored whether changes in the expression of these specific genes or other genes are the key drivers of the observed detrimental effect of H3K9cr. Owing to our ChIP-seq data and studies reporting the association between kidney injury and inflammation, cytokine IL-1β has become a subject of interest [38]. Previous studies

reported that the inhibition of IL-1β by human recombinant IL-1 receptor antagonist anakinra or antimurine IL-1β IgG could protect kidney inflammation and fibrosis; however, the mechanism is mainly limited to one type of cell [39,40]. Recently, a single-cell analysis revealed that inflammatory signaling connections were active in maladaptive TECs and myeloid cells, as well as among epithelial cells in fibrotic kidneys; IL-1β proved to be the important hub gene [17]. According to our data, tubular cell-derived IL-1β could stimulate M1 macrophage polarization to build a microinflammatory environment, which continue promoting persistent inflammation to damage tubular cells. Simultaneously, tubular cell-derived IL-1β could induce cellular senescence of TECs, as previously found in other cells [20,41]. Senescent TECs are then expressed and secrete a variety of SASPs that further mediate chronic inflammation and have profound effects on neighboring cells [42−44]. It is possible that the SASPs of senescent TECs might activate macrophages and induce their polarization towards the secretory M1 type to exacerbate the inflammatory environment, as observed in the liver [45]. The relationships between TECs and macrophages to maintain this vicious cycle of maladaptive repair in kidney fibrosis is complicated; however, IL-1β may be a potential central regulator [17]. In fact, our report does not provide detailed information about how IL-1β could trigger cellular senescence directly. Previous studies mentioned that the oxidative stress-dependent mechanism is how microglia-derived IL-1β induces p53 activation [46], and miR-103/107 expression is part of the p53 response triggered by secreted IL-1β that renders macrophages refractory to HIV-1 entry [47]. Particularly as the recent results of the canakinumab anti-inflammatory thrombosis outcomes study trial underscore the clinical efficacy of selective IL-1β inhibition in the prevention of cardiovascular adverse events after acute coronary syndrome [20]. Perhaps the pharmacological inhibition of IL-1β will represent an effective therapeutic tool for both cardiovascular disease and kidney fibrosis.

Presently, treatment for CKD is difficult, and the prognosis is difficult to determine. Our study identifies a potential clinical target to treat kidney fibrosis, besides the IL-1β mentioned above. The current therapeutic drugs for PTMs have certain positive effects under various pathological conditions, including renal injury [48]. It is encouraging that some epigenetic modifier drugs are already in clinical use or undergoing clinical trials, with some already reporting promising post hoc results (as is the case for apabetalone) [49,50]. However, most of our understanding of epigenetic modifiers and the kidneys is derived from the adverse effects of drugs already in clinical use for nonrenal indications [51,52]. ACSS2 inhibitors may be another promising target to modify histone Kcr, which has been studied in several other diseases and has already demonstrated benefits [53−58]. Conversely, the success of clinical senotherapeutic trials in patients with kidney disease highlighted another way to treat CKD by alleviating cellular senescence [59,60]. The discoveries in our present study have unique clinical relevance and physiological significance. Nevertheless, this promising field merits further research that should focus on drugs already in clinical use or undergoing clinical trials, as they are likely to eventually translate these advances to clinical practice within a more reasonable time than completely new molecular entities.

Limitations of our work include uncertainty regarding the importance and transferability of the ACSS2-H3K9cr-IL-1β axis from animals to humans. Although we show the data of human kidney slides and cells,

future studies need to confirm the importance of this axis using human kidney tissue. Another limitation is that the effect of pharmacological ACSS2 inhibition was examined using a single molecule. Testing multiple, well-characterized ACSS2 inhibitors with distinct chemical scaffolds would be warranted to mitigate the risk of off-target effects. Although we have shown that alterations of H3K9cr are positively associated with changes in gene expression during kidney fibrosis, and further demonstrated that histone Kcr is functionally important for this process, we did not analyze in detail how this modification relates to known chromatin states (active versus poised versus heterochromatin), and do not explore the roles of other Kcrs in this paper. Future studies are needed to better understand the correlational and causal relationships between histone Kcr and overall chromatin remodeling, as well as the correlation between different Kcrs during kidney fibrosis. Last, the mechanism by which IL-1β is secreted by tubular cells and transferred to macrophages was not investigated in this paper. Based on prior studies, we suggest that exosomes—enriched with miRNAs and mRNAs [61]—might act as cargo for intercellular communication to provide a novel mechanism of cross-talk between TECs and macrophages [62]; still, further research is required.

In conclusion, we reveal that the pattern of protein crotonylation changes during kidney fibrosis, suggesting a role of H3K9cr in kidney injury and fibrosis. The degree of kidney cell histone Kcr can be therapeutically manipulated by ACSS2 inhibitors, and decreasing H3K9cr-mediated macrophage polarization and tubular senescence is nephroprotective. Collectively, our findings uncover that H3K9 crotonylation plays a critical, previously unrecognized role in kidney fibrosis, where ACSS2 represents an attractive target for strategies that aim to slow fibrotic kidney disease progression. However, the precise mechanisms for the protective effect of H3K9cr remains to be further clarified.

Methods

Animals

The protocol of the animal research was reviewed and authorized by the Experimental Animal Ethics Committee of West China Hospital, Sichuan University (2022527004). ACSS2 knockout (KO) mice, C57BL/6J mice, and TEC- specific ACSS2 mice were acquired from Gempharmatech Co. Ltd. (Nanjing, China). All animals were randomly grouped (3–7 mice per group), and the procedures of the fibrosis model were performed according to the operating procedure described in the supplementary data.

Drug studies for *in vivo* experiments

For the inhibitor studies, littermate mice were randomly injected with either the ACSS2 inhibitor or antimurine IL-1β antibodies. The ACSS2 inhibitor (S8588, Selleck, Shanghai, China) was diluted in 0.9% saline, and orally administered at a dose of 50 mg/kg/d for 7 consecutive days after UUO surgery or FA injection. Seven days after surgery or FA injection, the mice were sacrificed. Antimurine IL-1β antibody or control IgG was administered at 10 mg/kg body weight intraperitoneally once a day for 7 consecutive days after UUO surgery. Mice were sacrificed on the 7th day after UUO surgery, and kidneys were

harvested. Procedures regarding the kidneys used for histologic examination and staining are described in the supplementary data.

Histone extraction and LC-MS/MS

To extract histones from kidneys, we first isolated the nuclei and proceeded with the acid-histone extraction method [63]. Two micrograms of histone lysates were loaded onto 15% SDS-PAGE gels; Coomassie brilliant blue was used for gel staining to demonstrate histone purification. Rest histone lysates were used for LC-MS/MS to double-check histone purification. Detailed information is presented in the supplementary data.

RNA and ChIP sequencing

Frozen kidney samples (n=3 per group) were randomly selected for sequencing. The construction and sequencing of libraries were conducted through LC-BIO Technology co., Ltd. (Hangzhou, China). ChIP assays were performed by Shandong Xiuyue Biotechnology Co., Ltd. (Shandong, China), according to the standard crosslinking ChIP protocol with modifications. Detailed information is presented in the supplementary data.

Statistical analysis

Statistical analysis was performed using the GraphPad Prism 9 software. One-way ANOVA and the unpaired t-test were performed on variables. Sample size estimation was not performed, and sample size was determined by the number of animals in the colony of a determined age and gender. The number of replicates (including the number of animals used in each experiment) are indicated in the figures and/or figure legends. All data are expressed as mean ± SEM. The statistical parameters can be found in the figures and the figure legends. $P < 0.05$ was considered significant. $P < 0.05$ (*), $P < 0.01$ (**), $P < 0.001$ (***) and $P < 0.0001$ (****).

Declarations

Data availability

The data that support the findings of this study are available from the corresponding author upon reasonable request.

Acknowledgments

Author contributions

L.L. and L.M designed the study. L.L., T.X., Y.W., S.T., and F.G. conducted the experiments. Y.W., and J.L. performed the bioinformatic analyses. L.L., T.X., and Y.W. analyzed the data. L.L. and L.M wrote the manuscript. H.F., and P.F. revised the language of the manuscript. All authors helped to interpret the results and approved the final version of the manuscript.

Competing interests

The authors declare that they have no competing interests.

References

1. Eckardt, K. U. *et al.* Evolving importance of kidney disease: from subspecialty to global health burden. Lancet 382, 158–169, doi:10.1016/S0140-6736(13)60439-0 (2013).
2. Webster, A. C., Nagler, E. V., Morton, R. L. & Masson, P. Chronic Kidney Disease. Lancet 389, 1238–1252, doi:10.1016/S0140-6736(16)32064-5 (2017).
3. National Kidney, F. KDOQI Clinical Practice Guideline for Diabetes and CKD: 2012 Update. Am J Kidney Dis 60, 850–886, doi:10.1053/j.ajkd.2012.07.005 (2012).
4. Kouzarides, T. Chromatin modifications and their function. Cell 128, 693–705, doi:10.1016/j.cell.2007.02.005 (2007).
5. Reddy, M. A. & Natarajan, R. Recent developments in epigenetics of acute and chronic kidney diseases. Kidney Int 88, 250–261, doi:10.1038/ki.2015.148 (2015).
6. Susztak, K. Understanding the epigenetic syntax for the genetic alphabet in the kidney. J Am Soc Nephrol 25, 10–17, doi:10.1681/ASN.2013050461 (2014).
7. Tan, M. *et al.* Identification of 67 histone marks and histone lysine crotonylation as a new type of histone modification. Cell 146, 1016–1028, doi:10.1016/j.cell.2011.08.008 (2011).
8. Ruiz-Andres, O. *et al.* Histone lysine crotonylation during acute kidney injury in mice. Dis Model Mech 9, 633–645, doi:10.1242/dmm.024455 (2016).
9. Lin, H. *et al.* Quantitative analysis of protein crotonylation identifies its association with immunoglobulin A nephropathy. Mol Med Rep 21, 1242–1250, doi:10.3892/mmr.2020.10931 (2020).
10. Bao, X. *et al.* Identification of 'erasers' for lysine crotonylated histone marks using a chemical proteomics approach. Elife 3, doi:10.7554/eLife.02999 (2014).
11. Wei, W. *et al.* Class I histone deacetylases are major histone decrotonylases: evidence for critical and broad function of histone crotonylation in transcription. Cell Res 27, 898–915, doi:10.1038/cr.2017.68 (2017).
12. Rousseaux, S. & Khochbin, S. Histone Acylation beyond Acetylation: Terra Incognita in Chromatin Biology. Cell J 17, 1–6, doi:10.22074/cellj.2015.506 (2015).
13. Sabari, B. R. *et al.* Intracellular crotonyl-CoA stimulates transcription through p300-catalyzed histone crotonylation. Mol Cell 58, 203–215, doi:10.1016/j.molcel.2015.02.029 (2015).

14. Yang, L., Besschetnova, T. Y., Brooks, C. R., Shah, J. V. & Bonventre, J. V. Epithelial cell cycle arrest in G2/M mediates kidney fibrosis after injury. *Nat Med* 16, 535–543, 531p following 143, doi:10.1038/nm.2144 (2010).

15. Gowans, G. J. *et al.* Recognition of Histone Crotonylation by Taf14 Links Metabolic State to Gene Expression. *Mol Cell* 76, 909–921 e903, doi:10.1016/j.molcel.2019.09.029 (2019).

16. Andrews, F. H. *et al.* The Taf14 YEATS domain is a reader of histone crotonylation. Nat Chem Biol 12, 396–398, doi:10.1038/nchembio.2065 (2016).

17. Balzer, M. S. *et al.* Single-cell analysis highlights differences in druggable pathways underlying adaptive or fibrotic kidney regeneration. Nat Commun 13, 4018, doi:10.1038/s41467-022-31772-9 (2022).

18. Lech, M. *et al.* Macrophage phenotype controls long-term AKI outcomes–kidney regeneration versus atrophy. J Am Soc Nephrol 25, 292–304, doi:10.1681/ASN.2013020152 (2014).

19. Han, L. *et al.* Interleukin-1beta-Induced Senescence Promotes Osteoblastic Transition of Vascular Smooth Muscle Cells. Kidney Blood Press Res 45, 314–330, doi:10.1159/000504298 (2020).

20. Shang, D., Hong, Y., Xie, W., Tu, Z. & Xu, J. Interleukin-1beta Drives Cellular Senescence of Rat Astrocytes Induced by Oligomerized Amyloid beta Peptide and Oxidative Stress. Front Neurol 11, 929, doi:10.3389/fneur.2020.00929 (2020).

21. Nakamura, Y., Aihara, R., Iwata, H., Kuwayama, T. & Shirasuna, K. IL1B triggers inflammatory cytokine production in bovine oviduct epithelial cells and induces neutrophil accumulation via CCL2. Am J Reprod Immunol 85, e13365, doi:10.1111/aji.13365 (2021).

22. Philipot, D. *et al.* p16INK4a and its regulator miR-24 link senescence and chondrocyte terminal differentiation-associated matrix remodeling in osteoarthritis. Arthritis Res Ther 16, R58, doi:10.1186/ar4494 (2014).

23. Xu, J., Zhou, L. & Liu, Y. Cellular Senescence in Kidney Fibrosis: Pathologic Significance and Therapeutic Strategies. Front Pharmacol 11, 601325, doi:10.3389/fphar.2020.601325 (2020).

24. Melk, A. *et al.* Expression of p16INK4a and other cell cycle regulator and senescence associated genes in aging human kidney. Kidney Int 65, 510–520, doi:10.1111/j.1523-1755.2004.00438.x (2004).

25. Sis, B. *et al.* Accelerated expression of senescence associated cell cycle inhibitor p16INK4A in kidneys with glomerular disease. Kidney Int 71, 218–226, doi:10.1038/sj.ki.5002039 (2007).

26. Braun, H. *et al.* Cellular senescence limits regenerative capacity and allograft survival. J Am Soc Nephrol 23, 1467–1473, doi:10.1681/ASN.2011100967 (2012).

27. Westhoff, J. H. *et al.* Hypertension induces somatic cellular senescence in rats and humans by induction of cell cycle inhibitor p16INK4a. Hypertension 52, 123–129, doi:10.1161/HYPERTENSIONAHA.107.099432 (2008).

28. Schroth, J., Thiemermann, C. & Henson, S. M. Senescence and the Aging Immune System as Major Drivers of Chronic Kidney Disease. Front Cell Dev Biol 8, 564461, doi:10.3389/fcell.2020.564461 (2020).

29. Li, S. *et al.* Glycoengineering of Therapeutic Antibodies with Small Molecule Inhibitors. Antibodies (Basel) 10, doi:10.3390/antib10040044 (2021).

30. Comerford, S. A. *et al.* Acetate dependence of tumors. Cell 159, 1591–1602, doi:10.1016/j.cell.2014.11.020 (2014).

31. Wang, H., Yang, Y., Liu, J. & Qian, L. Direct cell reprogramming: approaches, mechanisms and progress. Nat Rev Mol Cell Biol 22, 410–424, doi:10.1038/s41580-021-00335-z (2021).

32. Ko, Y. A. *et al.* Cytosine methylation changes in enhancer regions of core pro-fibrotic genes characterize kidney fibrosis development. Genome Biol 14, R108, doi:10.1186/gb-2013-14-10-r108 (2013).

33. Shiels, P. G., McGuinness, D., Eriksson, M., Kooman, J. P. & Stenvinkel, P. The role of epigenetics in renal ageing. Nat Rev Nephrol 13, 471–482, doi:10.1038/nrneph.2017.78 (2017).

34. Dang, L. *et al.* Nuclear Condensation of CDYL Links Histone Crotonylation and Cystogenesis in Autosomal Dominant Polycystic Kidney Disease. J Am Soc Nephrol 33, 1708–1725, doi:10.1681/ASN.2021111425 (2022).

35. Tang, X. *et al.* Short-Chain Enoyl-CoA Hydratase Mediates Histone Crotonylation and Contributes to Cardiac Homeostasis. Circulation 143, 1066–1069, doi:10.1161/CIRCULATIONAHA.120.049438 (2021).

36. Lu, Y. *et al.* Dynamics and functional interplay of histone lysine butyrylation, crotonylation, and acetylation in rice under starvation and submergence. Genome Biol 19, 144, doi:10.1186/s13059-018-1533-y (2018).

37. Fang, Y. *et al.* Histone crotonylation promotes mesoendodermal commitment of human embryonic stem cells. *Cell Stem Cell* 28, 748–763 e747, doi:10.1016/j.stem.2020.12.009 (2021).

38. Lemos, D. R. *et al.* Interleukin-1beta Activates a MYC-Dependent Metabolic Switch in Kidney Stromal Cells Necessary for Progressive Tubulointerstitial Fibrosis. J Am Soc Nephrol 29, 1690–1705, doi:10.1681/ASN.2017121283 (2018).

39. Shahzad, K. *et al.* Nlrp3-inflammasome activation in non-myeloid-derived cells aggravates diabetic nephropathy. Kidney Int 87, 74–84, doi:10.1038/ki.2014.271 (2015).

40. Lei, Y. *et al.* Interleukin-1beta Inhibition for Chronic Kidney Disease in Obese Mice With Type 2 Diabetes. Front Immunol 10, 1223, doi:10.3389/fimmu.2019.01223 (2019).

41. Sturmlechner, I., Durik, M., Sieben, C. J., Baker, D. J. & van Deursen, J. M. Cellular senescence in renal ageing and disease. Nat Rev Nephrol 13, 77–89, doi:10.1038/nrneph.2016.183 (2017).

42. Taddei, M. L. *et al.* Senescent stroma promotes prostate cancer progression: the role of miR-210. Mol Oncol 8, 1729–1746, doi:10.1016/j.molonc.2014.07.009 (2014).

43. Kang, T. W. *et al.* Senescence surveillance of pre-malignant hepatocytes limits liver cancer development. Nature 479, 547–551, doi:10.1038/nature10599 (2011).

44. Xue, W. *et al.* Senescence and tumour clearance is triggered by p53 restoration in murine liver carcinomas. Nature 445, 656–660, doi:10.1038/nature05529 (2007).

45. Huang, Y. *et al.* The hepatic senescence-associated secretory phenotype promotes hepatocarcinogenesis through Bcl3-dependent activation of macrophages. Cell Biosci 11, 173, doi:10.1186/s13578-021-00683-5 (2021).

46. Guadagno, J., Swan, P., Shaikh, R. & Cregan, S. P. Microglia-derived IL-1beta triggers p53-mediated cell cycle arrest and apoptosis in neural precursor cells. Cell Death Dis 6, e1779, doi:10.1038/cddis.2015.151 (2015).

47. Lodge, R. *et al.* Interleukin-1beta Triggers p53-Mediated Downmodulation of CCR5 and HIV-1 Entry in Macrophages through MicroRNAs 103 and 107. *mBio* 11, doi:10.1128/mBio.02314-20 (2020).

48. Van Beneden, K. *et al.* Comparison of trichostatin A and valproic acid treatment regimens in a mouse model of kidney fibrosis. Toxicol Appl Pharmacol 271, 276–284, doi:10.1016/j.taap.2013.05.013 (2013).

49. Ghosh, G. C., Bhadra, R., Ghosh, R. K., Banerjee, K. & Gupta, A. RVX 208: A novel BET protein inhibitor, role as an inducer of apo A-I/HDL and beyond. Cardiovasc Ther 35, doi:10.1111/1755-5922.12265 (2017).

50. Allison, S. Apabetalone in chronic kidney disease. Nat Rev Nephrol 17, 437, doi:10.1038/s41581-021-00443-1 (2021).

51. Ranganathan, P. *et al.* Histone deacetylase-mediated silencing of AMWAP expression contributes to cisplatin nephrotoxicity. Kidney Int 89, 317–326, doi:10.1038/ki.2015.326 (2016).

52. Kulikowski, E. *et al.* Sp425effects of Apabetalone (Rvx-208) on Serum Albumin in Subjects with Cvd, Diabetes and Chronic Kidney Disease; a Post-Hoc Analysis of the Assure and Sustain Clinical Trials. Nephrology Dialysis Transplantation 32, iii264-iii264, doi:10.1093/ndt/gfx149 (2017).

53. Miller, K. D. *et al.* Targeting ACSS2 with a Transition-State Mimetic Inhibits Triple-Negative Breast Cancer Growth. Cancer Res 81, 1252–1264, doi:10.1158/0008-5472.CAN-20-1847 (2021).

54. Li, Z. *et al.* Acetyl-CoA Synthetase 2: A Critical Linkage in Obesity-Induced Tumorigenesis in Myeloma. *Cell Metab* 33, 78–93 e77, doi:10.1016/j.cmet.2020.12.011 (2021).

55. Sabnis, R. W. Novel Substituted Tetrazoles as ACSS2 Inhibitors for Treating Cancer. ACS Med Chem Lett 12, 1894–1895, doi:10.1021/acsmedchemlett.1c00621 (2021).

56. Jiang, G. *et al.* HIV latency is reversed by ACSS2-driven histone crotonylation. J Clin Invest 128, 1190–1198, doi:10.1172/JCI98071 (2018).

57. Calhoun, S., Duan, L. & Maki, C. G. Acetyl-CoA synthetases ACSS1 and ACSS2 are 4-hydroxytamoxifen responsive factors that promote survival in tamoxifen treated and estrogen deprived cells. Transl Oncol 19, 101386, doi:10.1016/j.tranon.2022.101386 (2022).

58. Li, X., Qian, X. & Lu, Z. Local histone acetylation by ACSS2 promotes gene transcription for lysosomal biogenesis and autophagy. Autophagy 13, 1790–1791, doi:10.1080/15548627.2017.1349581 (2017).

59. Torres, B. *et al.* Impact of switching to raltegravir and/or adding losartan in lymphoid tissue fibrosis and inflammation in people living with HIV. A randomized clinical trial. HIV Med 22, 674–681, doi:10.1111/hiv.13114 (2021).

60. Hickson, L. J. *et al.* Senolytics decrease senescent cells in humans: Preliminary report from a clinical trial of Dasatinib plus Quercetin in individuals with diabetic kidney disease. EBioMedicine 47, 446–456, doi:10.1016/j.ebiom.2019.08.069 (2019).

61. Lv, L. L. *et al.* Exosomal CCL2 from Tubular Epithelial Cells Is Critical for Albumin-Induced Tubulointerstitial Inflammation. J Am Soc Nephrol 29, 919–935, doi:10.1681/ASN.2017050523 (2018).

62. Li, Z. L. *et al.* HIF-1alpha inducing exosomal microRNA-23a expression mediates the cross-talk between tubular epithelial cells and macrophages in tubulointerstitial inflammation. Kidney Int 95, 388–404, doi:10.1016/j.kint.2018.09.013 (2019).

63. Zhao, S. *et al.* ATP-Citrate Lyase Controls a Glucose-to-Acetate Metabolic Switch. Cell Rep 17, 1037–1052, doi:10.1016/j.celrep.2016.09.069 (2016).

Figures
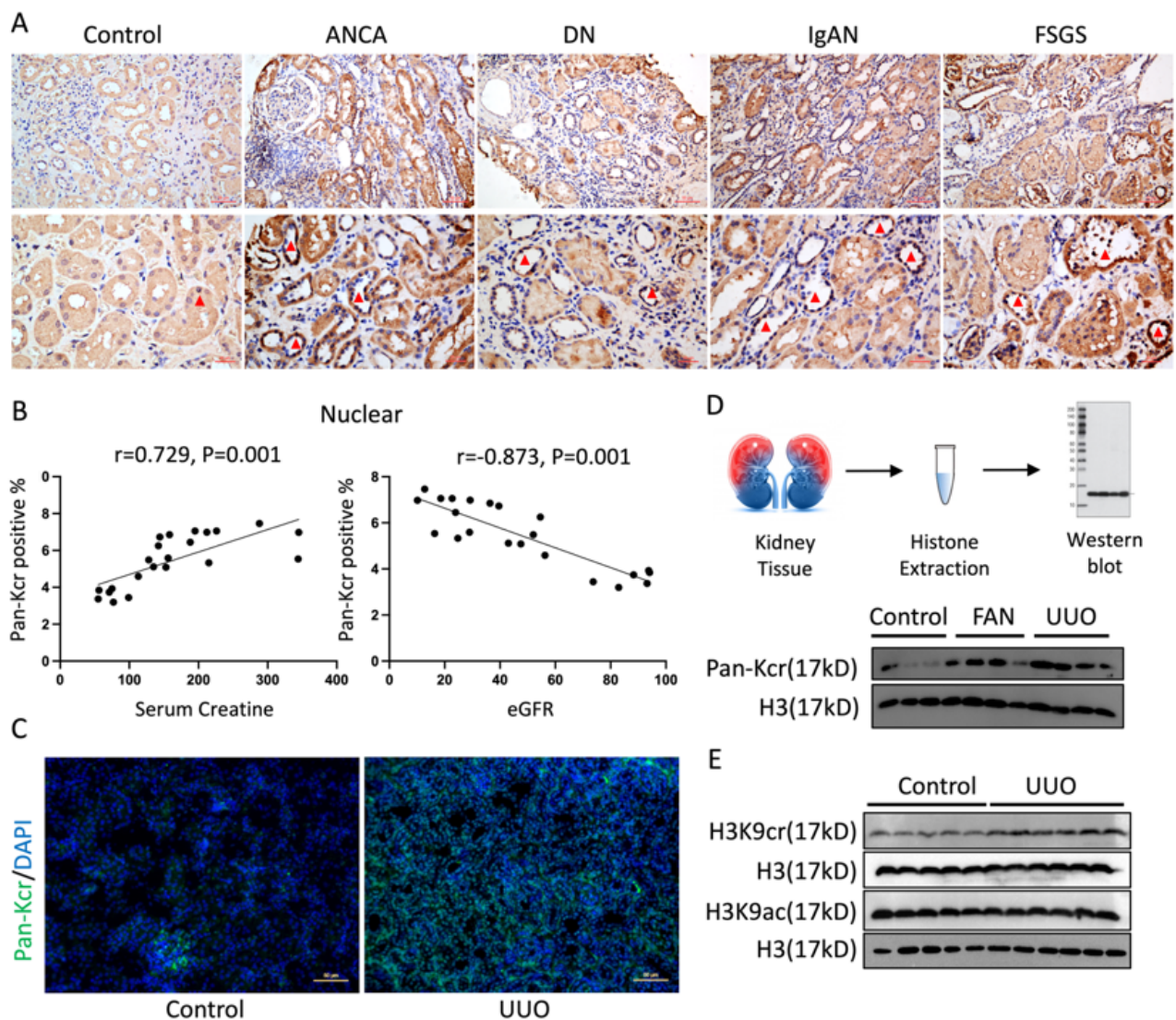
Figure 1

Histone Kcr expression positively correlates with disease severity in patients and mice with CKD. (A) Representative immunohistochemical (IHC) staining of anticrotonyllysine (pan-Kcr) antibody in healthy control subjects and patients with CKD. (B) Quantitative IHC analysis of pan-Kcr expression in controls and patients with CKD using ImageJ 6.0 software. (C) Immunofluorescence (IF) staining of pan-Kcr (green) and DAPI (blue) in control and UUO kidneys. (D) Flow chart of process to collect histone and protein expression data for histone crotonylation in the fibrotic kidneys of mice. (E) Protein expression of H3K9cr, H3K9ac, and H3 in the fibrotic kidneys of mice with UUO were determined by western blotting (n = 5 to 6 animals per group). Statistical analysis by Pearson correlation.
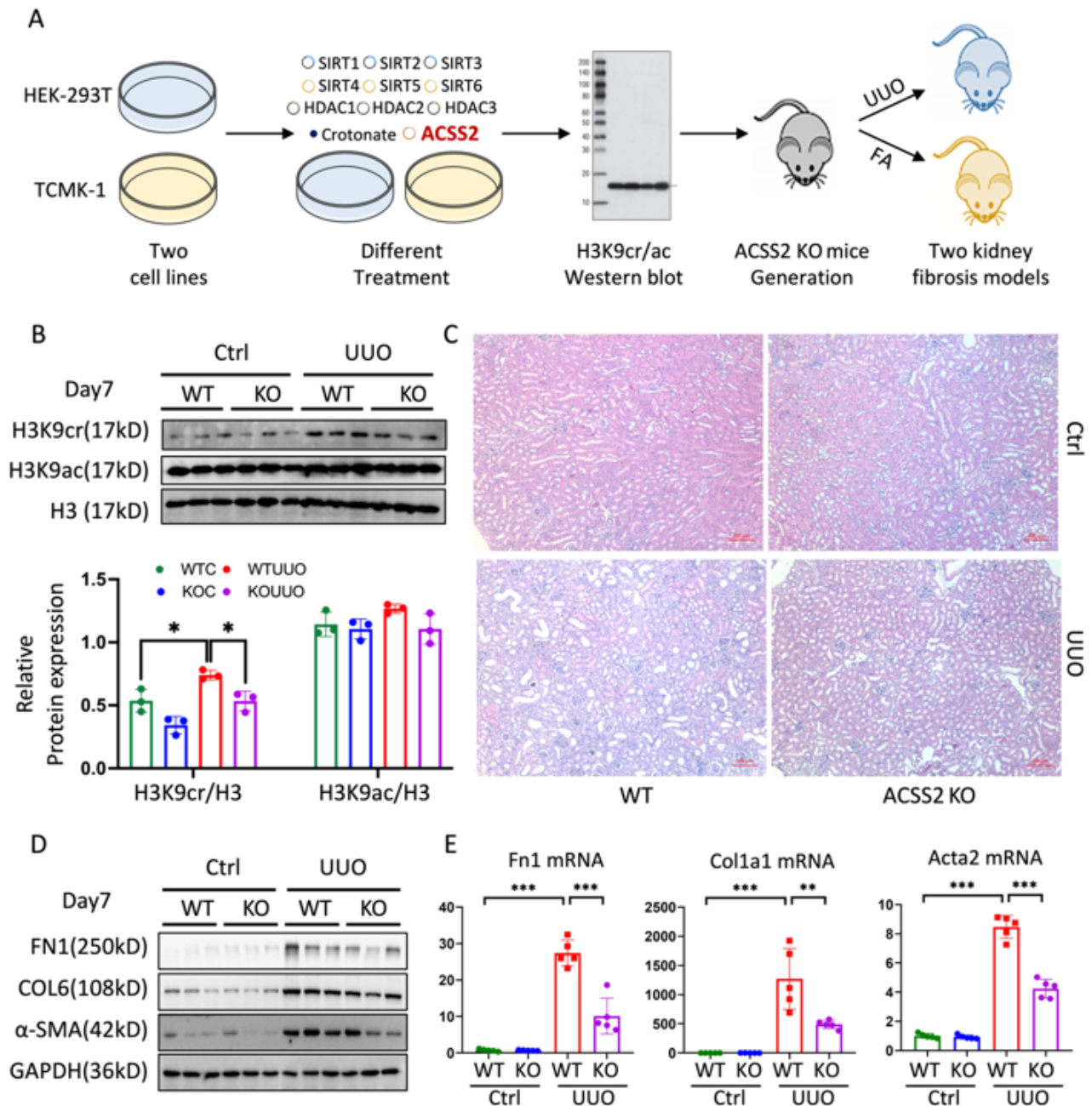
Figure 2

Global genetic deletion of ACSS2 suppressed H3K9cr expression and alleviated kidney fibrosis in mice.

(A) Schematic overview of the process for screening factors influencing H3K9cr *in vitro*, and experimental design in ACSS2 $^{-/-}$ UUO/FAN mice. (B) Protein expression and quantitative analysis of H3K9cr, H3K9ac, and H3 in whole kidney lysates of UUO mice (n = 3 per group). (C) Representative images of H&E staining in UUO mice. (D) FN1, COL6, α-SMA and GAPDH immunoblotting in whole kidney lysates of UUO mice (n = 3 per group). (E) The mRNA levels of Fn1, Col1a1, and Acta2 in whole kidney lysates of UUO mice (n = 5 per group). Data shown are means ± SEM. Statistical analysis by one-way ANOVA with Tukey's post hoc test. ** P < 0.01 and *** P < 0.001.
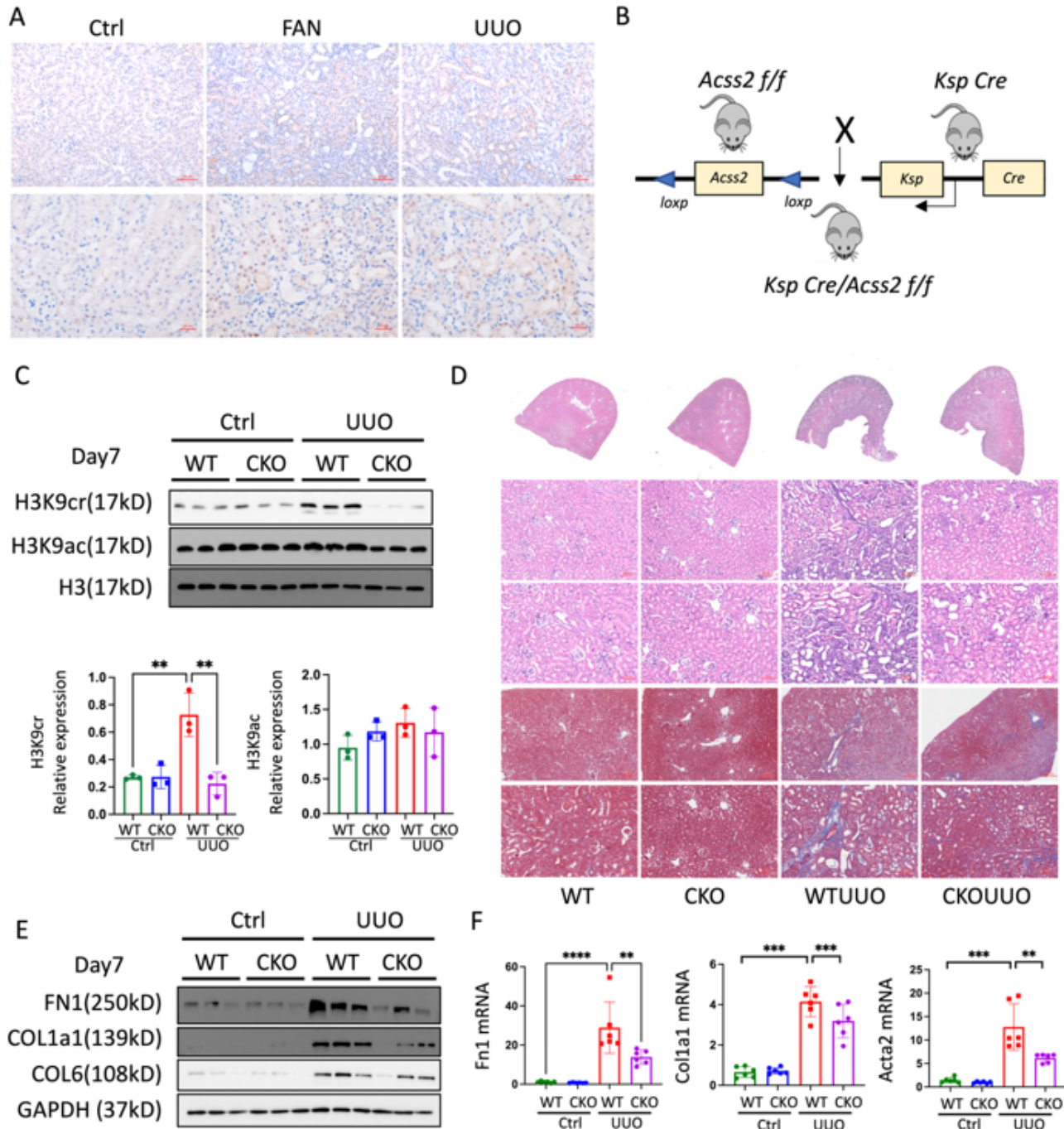
Figure 3

TEC-specific knockout of ACSS2 suppressed H3K9cr expression and alleviated kidney fibrosis in mice. (A) Representative IHC staining of ACSS2 in controls and experimental mice (with UUOs or injected with FA). (B) Design strategy of TEC-specific ACSS2 KO (ACSS2^{tecKO}) mice. (C) H3K9cr, H3K9ac, and H3 immunoblotting, and quantification of these immunoblots in the whole kidney lysates of ACSS2^{tecKO} mice (n = 3 per group). (D) Representative images of H&E and Masson staining in ACSS2^{tecKO} mice. (E) FN1, COL1a1, COL6, and GAPDH immunoblotting in the whole kidney lysates of ACSS2^{tecKO} mice (n = 3 per group). (F) mRNA levels of Fn1, Col1a1, Acta2, or Col6 in whole kidney lysates of WT and ACSS2^{tecKO} mice with UUOs (n = 6 per group). Data are shown as means ± SEM. Statistical analysis was performed via one-way ANOVA with Tukey's post hoc test. ** $P < 0.01$, *** $P < 0.001$ and **** $P < 0.0001$.
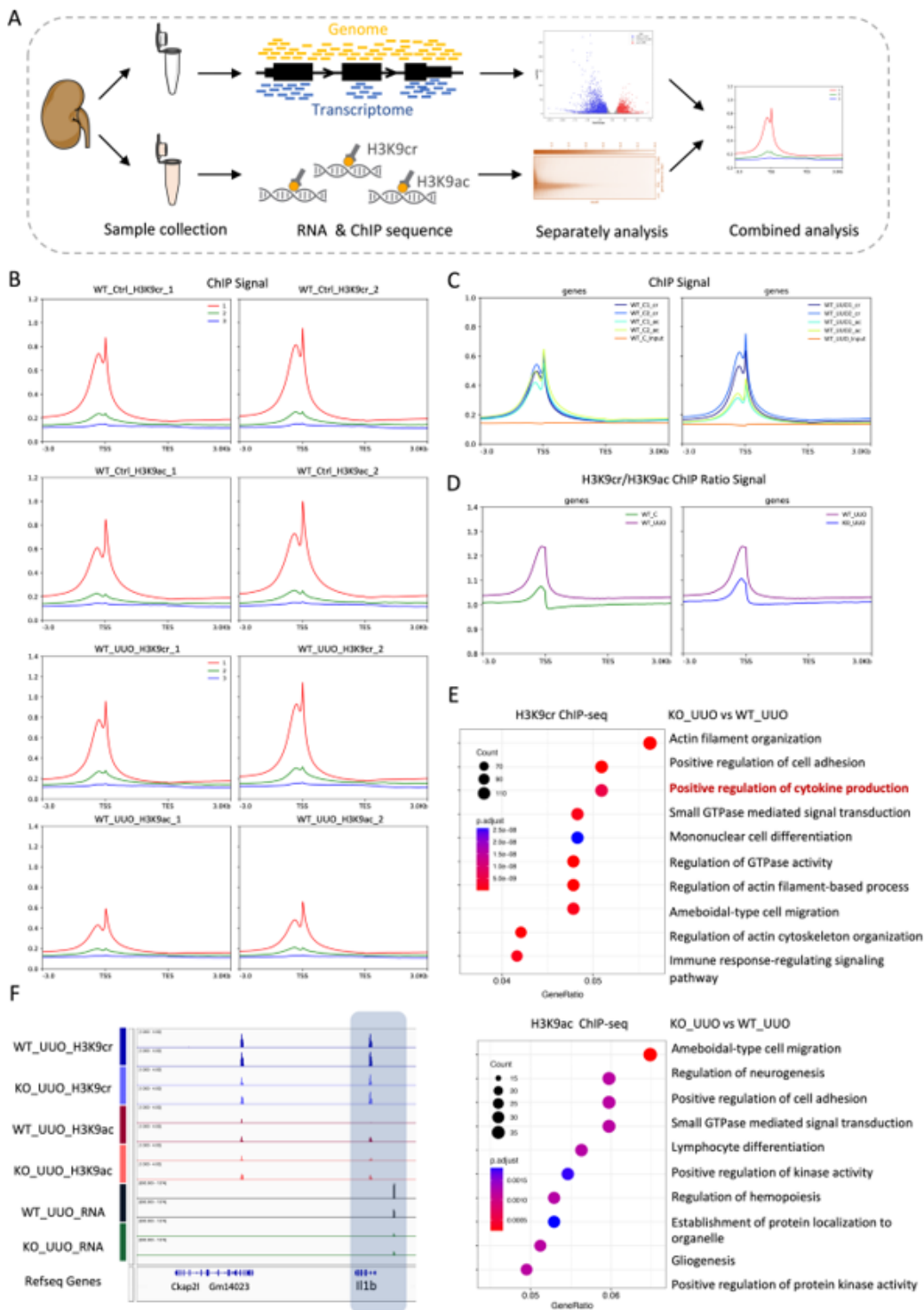
Figure 4

Combination analysis of ChIP-seq and RNA-seq in kidneys of ACSS2$^{-/-}$ UUO mice. (A) Outline of bioinformatic analysis strategy. (B) All genes were split into three equal groups based on their expression levels, calculated using RNA-seq. Mean H3K9cr and H3K9ac ChIP signals are shown for each quartile of gene expression, and are shown using different colored lines (the red line is the gene with the highest, and the blue line with the lowest expression) in both control and UUO mice. (C) H3K9cr, H3K9ac, and input

ChIP signals are shown in both control and UUO mice. TSS, transcriptional start site; TES, transcriptional termination site. (D) Mean H3K9cr to H3K9ac ChIP ratios in the control and UUO groups of WT and ACSS2$^{-/-}$ mice. (E) Comparable analysis of ChIP-seq data between WT and ACSS2$^{-/-}$ UUO mice using GO database. (F) Genome browser representation of RNA-seq reads and ChIP-seq reads for Il1b in control and ACSS2$^{-/-}$ UUO mice.
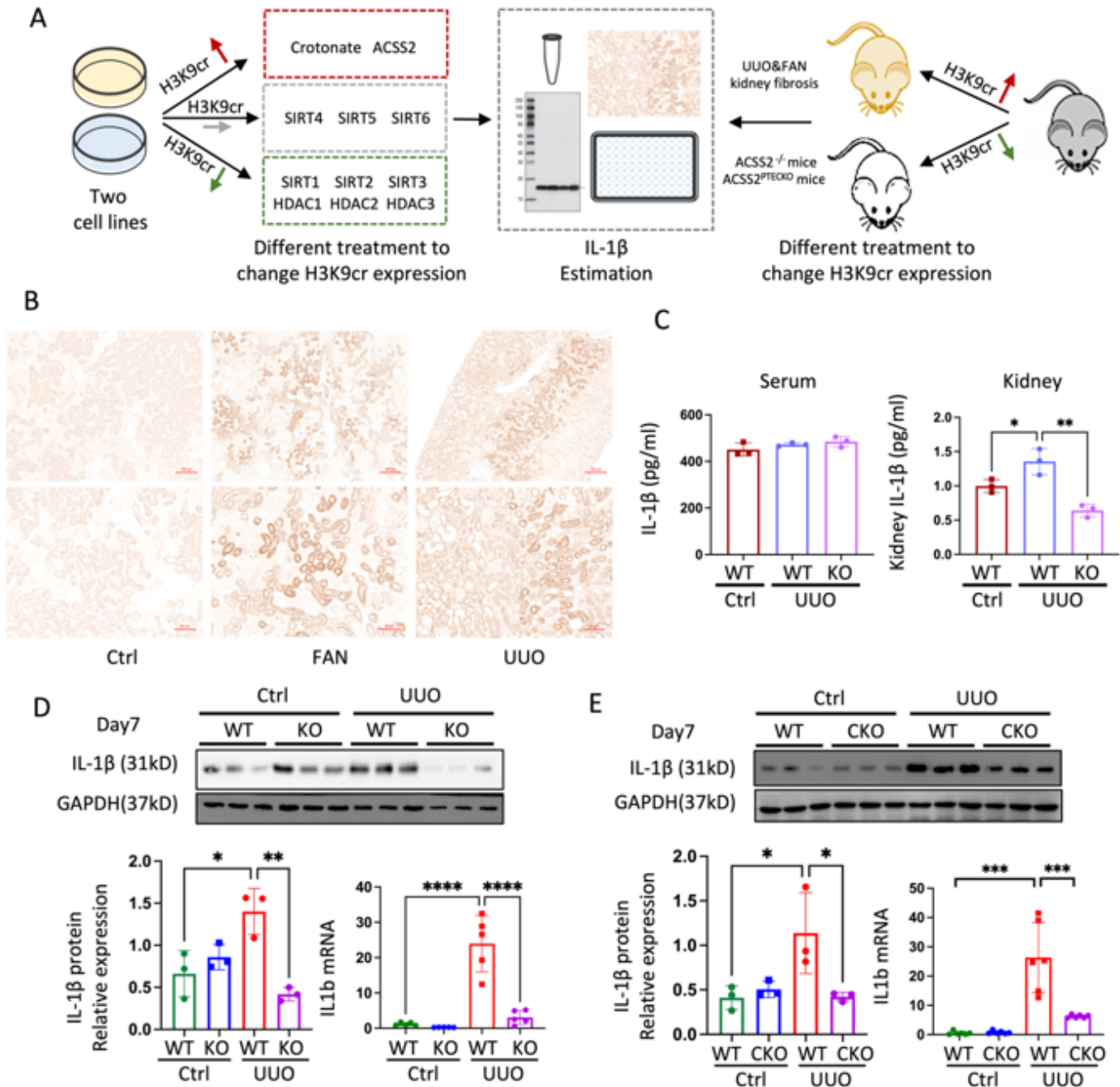

Figure 5

Changes in H3K9cr-mediated IL-1β expression under different conditions. (A) Schematic overview of the process for screening changes in IL-1β both *in vivo* and *in vitro*. (B) Representative immunohistochemical

stain of IL-1β in mice with UUOs or injected with FA. (C) IL-1β concentration of serum and kidneys in WT and ACSS2$^{-/-}$ mice, measured by ELISA kit (n = 3 per group). (D) IL-1β immunoblotting and quantification of IL-1β immunoblots normalized to GAPDH, as well as Il1b mRNA levels in ACSS2$^{-/-}$ mice (n = 3 per group). (E) IL-1β immunoblotting and quantification of IL-1β immunoblots normalized to GAPDH, as well as Il1b mRNA levels in ACSS2^{tecKO} mice (n = 3 per group). Data shown are means ± SEM. Statistical analysis by one-way ANOVA with Tukey's post hoc test. * P < 0.05, ** P < 0.01, *** P < 0.001 and **** P < 0.0001.
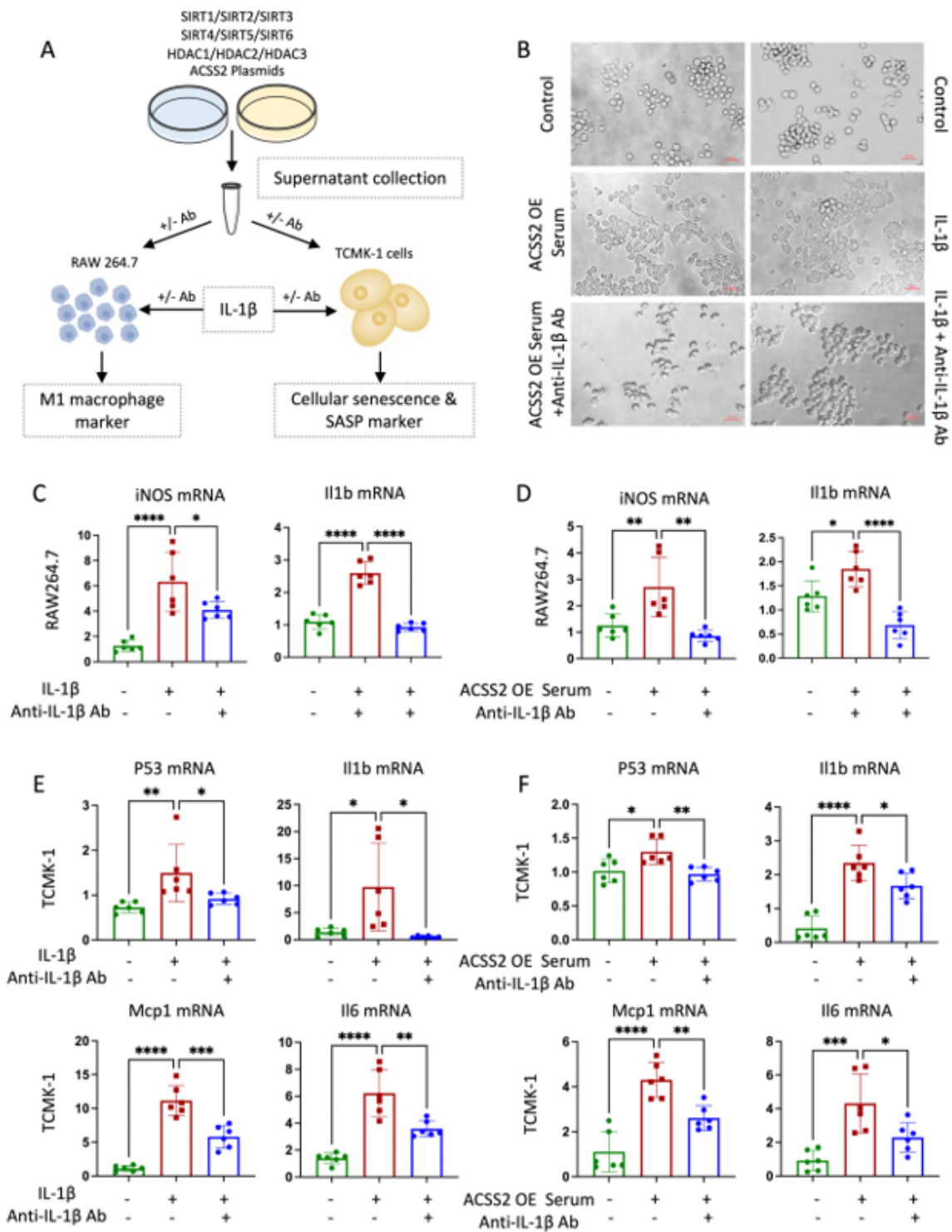
Figure 6

H3K9cr-derived IL-1β production triggered macrophage activation and tubular senescence, which could be neutralized by anti-IL-1β IgG. (A) Schematic overview of the process for researching the effects of H3K9cr-derived IL-1β on macrophage and tubular cells. (B) Microscopic images depicting the morphology changes in RAW264.7 cells after stimulation with IL-1β (5 ng/ml), or supernatants collected from HEK-293T cells transfected with ACSS2 plasmids. IL-1β antibody (5 μg/ml), added to neutralize supernatants

or IL-1β, inverted the morphological changes. (C) iNOS and Il1b mRNAs of RAW264.7, which were stimulated by IL-1β with or without IL-1β antibody neutralization (n = 6 per group). (D) iNOS and Il1b mRNAs of RAW264.7, which were stimulated using supernatants from HEK-293T cells transfected with ACSS2 plasmids with or without IL-1β antibody neutralization (n = 6 per group). (E) P53, Il1b, Il6, and Mcp1 mRNA levels of TCMK-1 cells, which were stimulated by IL-1β (5 μg/ml) with or without IL-1β antibody neutralization (5 μg/ml) (n = 6 per group). (F) P53, Il1b, Il6, and Mcp1 mRNA levels of TCMK-1 cells stimulated with supernatants from HEK-293T cells transfected with ACSS2 plasmids with or without IL-1β antibody neutralization (n = 6 per group). Data shown are means ± SEM. Statistical analysis was performed using one-way ANOVA with Tukey's post hoc test. * P < 0.05, ** P < 0.01, *** P < 0.001 and **** P < 0.0001.
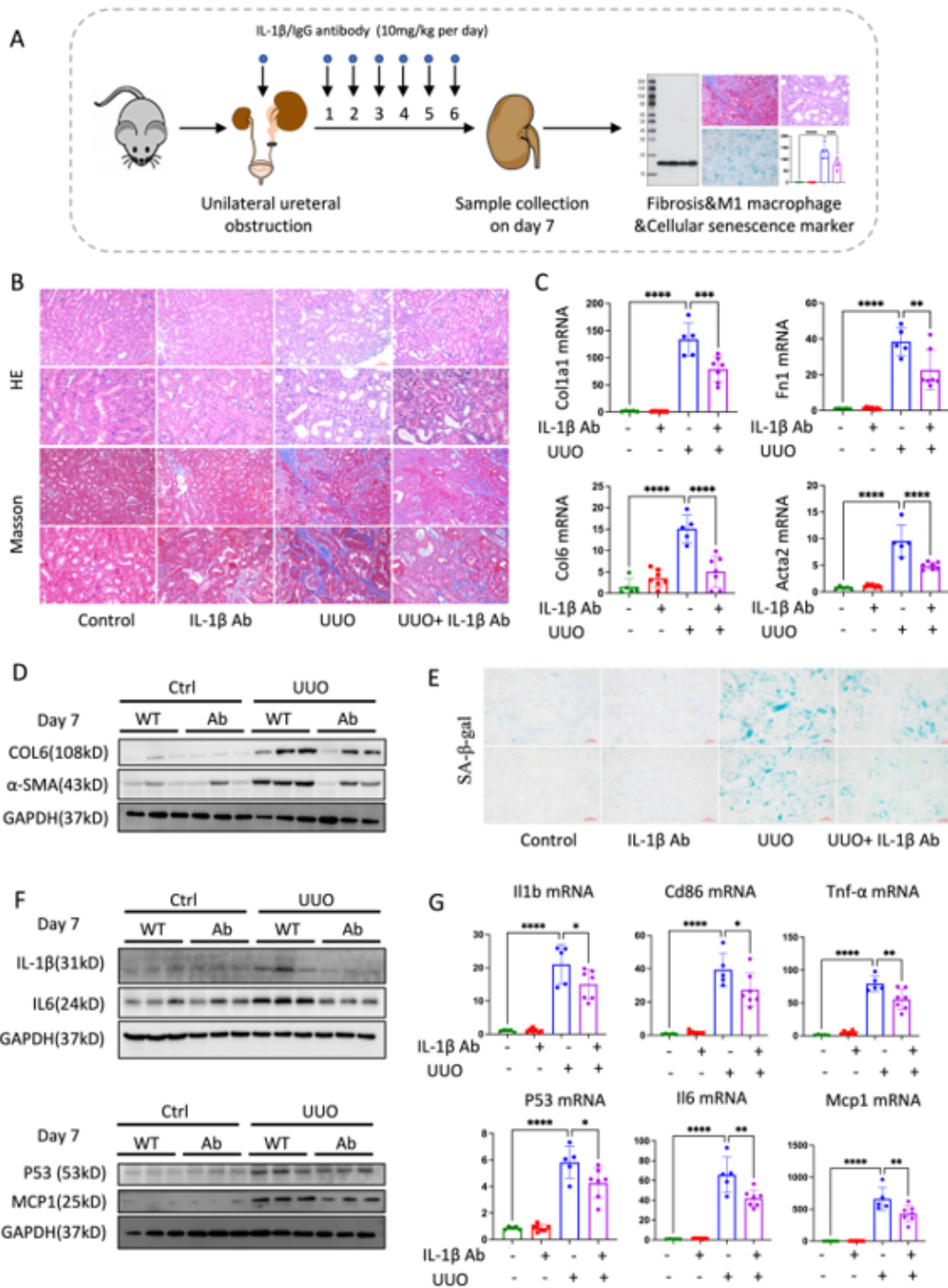
Figure 7

Anti-IL-1β IgG treatment decreased cellular senescence and M1 macrophage markers, and alleviated kidney fibrosis in mice. (A) Anti-IL-1β IgG treatment strategy for mice. (B) Representative images of H&E and Masson staining in the kidneys of UUO mice treated with IL-1β antibodies (10 mg/kg). (C) Fn1, Col1a1, Col6, and Acta2 mRNA levels in whole kidney lysates of UUO mice treated with IL-1β antibodies (10 mg/kg) (n = 5 to 7 per group). (D) COL6, α-SMA, and GAPDH immunoblotting in whole kidney lysates

of UUO mice treated with IL-1β antibodies (10 mg/kg) (n = 3 per group). (E) SA-β-gal staining in UUO mice treated with IL-1β antibodies (10 mg/kg). (F) IL-1β, IL6, P53, MCP1, and GAPDH immunoblotting in UUO mice neutralized with IL-1β antibodies (n = 3 per group). (G) Il1b, Cd86, Tnf-α, P53, Il6, and Mcp1 mRNA levels in UUO mice treated with IL-1β antibodies (10 mg/kg) (n = 5 to 7 per group). Data shown are means ± SEM. Statistical analysis by one-way ANOVA with Tukey's post hoc test. * P < 0.05, ** P < 0.01, *** P < 0.001 and **** P < 0.0001.
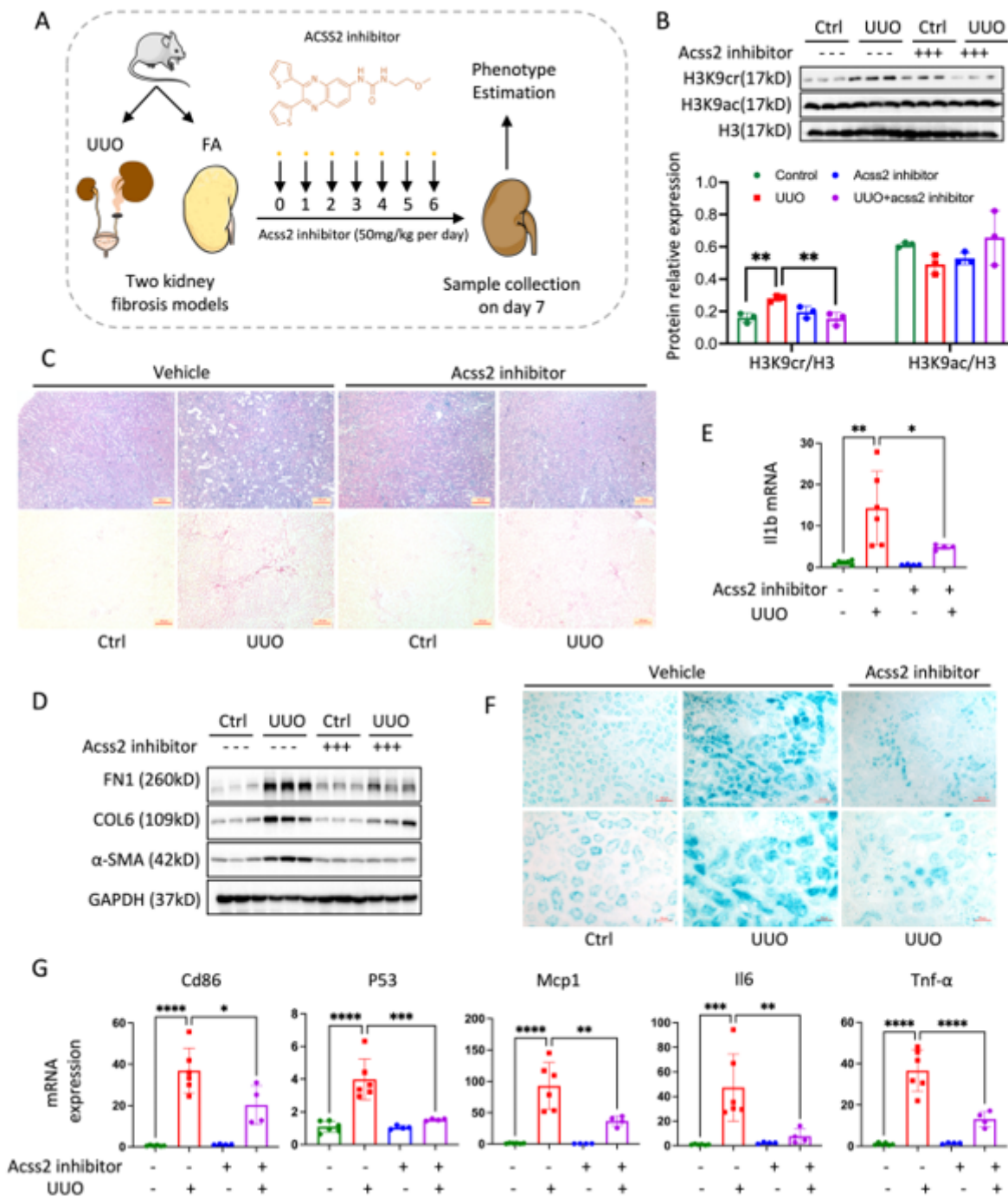

Figure 8

The ACSS2 inhibitor suppressed H3K9cr-mediated IL-1β expression, decreased cellular senescence, and M1 macrophage markers, and alleviated kidney fibrosis in mice. (A) ACSS2 inhibitor treatment strategy in UUO and FAN mice. (B) Protein expression of H3K9cr, H3K9ac, and H3, and quantification of these immunoblots in whole kidney lysates of UUO mice treated with or without ACSS2 inhibitors (n = 3 per group). (C) Representative images of H&E and Sirus red staining in UUO mice treated with or without ACSS2 inhibitors. (D) FN1, COL6, α-SMA, and GAPDH immunoblotting in whole kidney lysates of UUO mice treated with or without ACSS2 inhibitors (n = 3 per group). (E) mRNA levels of Il1b in whole kidney lysates of UUO mice treated with or without ACSS2 inhibitors (n = 4 to 6 per group). (F) SA-β-gal staining of control, UUO fibrotic, and UUO mice treated with ACSS2 inhibitors. (G) mRNA levels of Cd86, P53, Mcp1, Il6, and Tnf-α in whole kidney lysates of control, UUO fibrotic, and UUO mice treated with ACSS2 inhibitors (n = 4 to 6 per group). Data are shown as means ± SEM. Statistical analysis performed using one-way ANOVA with Tukey's post hoc test. *P < 0.05, ** P < 0.01, *** P < 0.001 and **** P < 0.0001.

Supplementary Files

This is a list of supplementary files associated with this preprint. Click to download.

- SupplementaryDatafinal.docx